

# Telomerization of 1,3-Butadiene with Biomass-Derived Alcohols over a Heterogeneous Pd/TPPTS Catalyst Based on Layered Double Hydroxides

A. N. Parvulescu,<sup>†</sup> P. J. C. Hausoul,<sup>†,‡</sup> P. C. A. Bruijninx,<sup>†</sup> S. T. Korhonen,<sup>†</sup> C. Teodorescu,<sup>§</sup> R. J. M. Klein Gebbink,<sup>‡</sup> and B. M. Weckhuysen<sup>\*,†</sup>

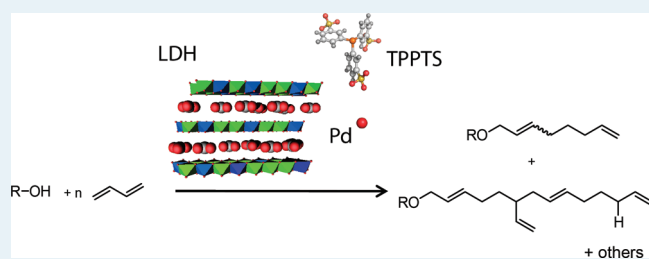
<sup>†</sup>Inorganic Chemistry and Catalysis group, Debye Institute for Nanomaterials Science, Utrecht University, Sorbonnelaan 16, 3584 CA Utrecht, The Netherlands

<sup>‡</sup>Organic Chemistry and Catalysis group, Debye Institute for Nanomaterials Science, Utrecht University, Padualaan 8, 3584 CH Utrecht, The Netherlands

<sup>§</sup>The National Institute of Materials Physics, Atomistilor Str. 105bis, P.O. Box MG. 7, 077125, Magurele-Bucharest, Romania

## Supporting Information

**ABSTRACT:** The telomerization of 1,3-butadiene with homogeneous palladium/phosphine catalysts is an efficient method to transform biomass-based oxygenates into useful fine and bulk chemicals, e.g. surfactants. Recovery and reuse of the expensive noble metal-based catalyst is highly desired for these systems and therefore a heterogeneous telomerization catalyst would be preferred. Layered double hydroxides (LDH) were investigated as supports for the heterogenization of the Pd/TPPTS (trisodium salt of 3,3',3''-phosphanetriyl benzene sulfonic acid) telomerization catalyst. Turn over numbers (TONs) up to 1300 were obtained with heterogeneous (immobilized palladium and ligand) and pseudo-heterogeneous (immobilized ligand) catalysts in the telomerization of 1,3-butadiene with ethylene glycol (EG) and methanol (MeOH) under solvent- and base-free conditions; TONs are comparable to those obtained with the homogeneous catalysts under similar conditions. Importantly, the LDH support was found to induce a change in product selectivity. In addition to the expected C8 telomers, higher telomers with C16 or C24 chains were observed with rather high selectivities (up to 48% for EG and 77% for MeOH).



**KEYWORDS:** telomerization, palladium, heterogeneous catalysis, layered double hydroxides, phosphines, biomass

## INTRODUCTION

Telomerization of 1,3-dienes is an efficient method for the synthesis of new C–C bonds. The catalytic reaction involves the dimerization of 1,3-dienes with the addition of a nucleophile and results in the formation of a telomer in a theoretically 100% atom-efficient process.<sup>1–8</sup> Furthermore, in the context of sustainable chemistry, the telomerization reaction is increasingly explored as a potential route for the valorization of biomass-derived feedstocks, such as glycerol, glycols, carbohydrates, starch, and phenols, into valuable products that can be used as intermediates for the production of surfactants, cosmetics, pharmaceuticals, and polymer components.<sup>2–13</sup>

Traditionally, the telomerization of 1,3-butadiene is catalyzed by homogeneous Pd-complexes with phosphine-based ligands, and, more recently, Pd-complexes with carbene ligands were also shown to be very active telomerization catalysts.<sup>2–8</sup> Although the telomerization of 1,3-butadiene provides an economically attractive route for the production of C8 bulk chemicals and is industrially applied for the production of 1-octanol and 1-octene,<sup>14,15</sup> there are still some major challenges that need to be addressed. One of these involves the recovery and reuse of the

homogeneous catalyst. Since expensive noble metals and phosphine ligands are used, the recovery of the catalyst materials as well as the purification of the reaction products is a difficult and often costly process.

There are a few reported examples of catalyst systems that aimed to solve this problem by either using a liquid–liquid biphasic process, or by attempting the development of a heterogeneous telomerization catalyst. An example of the former approach<sup>2,5,16–18</sup> was to use the water-soluble Pd/TPPTS (trisodium salt of 3,3',3''-phosphanetriyl benzene sulfonic acid) telomerization catalyst in a biphasic reaction system. It was thus possible to recover the telomerization catalyst in the water layer, but leaching of Pd into the organic phase as well as catalyst deactivation was observed. The leaching of palladium into the organic phase could in some cases be reduced by using additives (e.g., cyclodextrins) or co-solvents (e.g., 2-octanol or 2-propanol).<sup>18</sup> Alternatively, the use of a heterogeneous telomerization catalyst may bring several

Received: December 29, 2010

Revised: March 13, 2011

Published: March 23, 2011

advantages, such as facile separation from the reaction mixture and the possibility of recycling. However, there are only few examples of heterogeneous telomerization catalysts, and all of them suffer from significant drawbacks such as instability because of metal or ligand leaching and a lower activity compared to the homogeneous catalyst. Most of the reported examples involve Pd immobilization on various organic polymers or inorganic solids, such as silica or  $\text{KF}/\text{Al}_2\text{O}_3$ .<sup>19–24</sup> Estrine et al. for instance studied the telomerization of butadiene with methanol and phenol using a Pd/TPPTS on  $\text{KF}/\text{Al}_2\text{O}_3$  catalyst, with turn over numbers (TONs) of up to 440 with methanol.<sup>20,24</sup> Often only either the ligand or the metal is supported, and the other component is added in solution. Furthermore, the use of solvents and/or base additives such as sodium methoxide or organic amines is often required, which results in excessive waste formation. This is clearly not desired from an environmental point of view.<sup>2–8</sup> There is therefore a clear need to study and develop new telomerization catalysts, in particular heterogeneous catalysts that will work under solvent-free conditions and in the absence of base additives.

Recently, we have reported on the catalytic activity of a Pd/TOMPP (with TOMPP = tris(2-methoxyphenyl)phosphine) system in the telomerization of 1,3-butadiene with various biomass-derived substrates, such as glycerol, glycols, sugars, and sugar alcohols.<sup>9–13</sup> We have shown that Pd/TOMPP is an exceptionally active telomerization catalyst capable of the solvent- and base-free conversion of a wide range of polyfunctional alcohols with very high TONs and turn over frequencies (TOFs). However, the development of a reaction system that will allow full recovery and reuse of the catalyst still needs to be addressed. Here, we extend our studies to the immobilization of a Pd/TPPTS catalyst system on a layered double hydroxide (LDH) support material through ion-exchange. The beneficial effect of the LDH support on the catalytic activity of the Pd/TPPTS system in the solvent- and soluble base-free liquid phase telomerization of 1,3-butadiene with biomass-based alcohols is explored. Immobilization of the catalyst on the LDH support shows a remarkable shift in product selectivity from classical C8 telomers to higher telomers.

## EXPERIMENTAL SECTION

**1. Catalysts Synthesis.** All chemicals were used as received:  $\text{Al}(\text{NO}_3)_3 \cdot 6\text{H}_2\text{O}$  (Acros, >99%),  $\text{Mg}(\text{NO}_3)_2 \cdot 9\text{H}_2\text{O}$  (Acros, >99%), NaOH (Acros, >99%),  $\text{AlCl}_3$  (Aldrich, >99%),  $\text{MgCl}_2 \cdot 6\text{H}_2\text{O}$  (Acros, 99%),  $\text{Ni}(\text{NO}_3)_2$  (Acros Organics, 99%),  $\text{NiCl}_2 \cdot 6\text{H}_2\text{O}$  (Fluka 99%), urea (Acros Organics, 99.5%), ethylene glycol (Aldrich, >99%), methanol (Aldrich, >99%), 1,3-butadiene (Linde),  $\text{Pd}(\text{acac})_2$  (Aldrich, 99%),  $\text{Pd}(\text{OAc})_2$  (Aldrich, >99%),  $\text{Pd}(\text{dba})_2$  (Aldrich), TPPTS (Strem Chemicals, 85 wt %),  $\text{MgAl}-\text{CO}_3$  Pural (MG 61T) (Sasol).

The layered double hydroxides were prepared by following procedures described in literature. Please see the Results and Discussion section for an explanation of the abbreviations used for compositions of the different LDHs.  $\text{MgAl}-\text{NO}_3/\text{CO}_3$  LDH was prepared<sup>25</sup> in a 1 L glass beaker, where 100 mL of deionized and degassed water was brought to a pH of 10 with NaOH and kept under an Ar flow (100 mL/min). A solution of 120 mL of 0.33 M  $\text{Al}(\text{NO}_3)_3 \cdot 6\text{H}_2\text{O}$  was simultaneously added together with 120 mL of 0.67 M  $\text{Mg}(\text{NO}_3)_2$  under a flow of Ar and vigorous stirring at room temperature. During the synthesis the pH of the solution was maintained at 10 by dropwise addition of

NaOH (1 M). The suspension was further stirred for 48 h at room temperature, and the white precipitate was centrifuged and washed several times with 1.5 L of degassed and deionized water. The resulting LDH was then dried under a flow of  $\text{N}_2$  at room temperature.

$\text{MgAl}-\text{Cl}/\text{CO}_3$  LDH was prepared following a similar synthesis procedure as for the  $\text{MgAl}-\text{NO}_3$  LDH with the difference that the suspension was heated to 333 K for 24 h. The white powder was also separated by centrifugation and washed with 1.5 L of degassed and deionized water, and the solid was dried under a  $\text{N}_2$  flow at room temperature.

$\text{NiAl}-\text{Cl}/\text{CO}_3$  LDH was prepared following a reported synthesis procedure, using  $\text{NiCl}_2$  and  $\text{AlCl}_3$  as the metal precursors.<sup>26</sup> The synthesis of the LDH was performed in 0.1 L of distilled water under vigorous stirring. The total concentration of metal ions in the solution was 0.5 mol/L, and the Ni/Al molar ratio was 2.0. Urea (1.65 mol/L) was used to keep the pH around 9. The reaction mixture was heated at 353 K under vigorous stirring for 39 h.  $\text{NiAl}-\text{NO}_3/\text{CO}_3$  was prepared from  $\text{Ni}(\text{NO}_3)_2$  and  $\text{Al}(\text{NO}_3)_3$  following a similar procedure, but the reaction mixture was stirred for 72 h instead.

The immobilization of the Pd/TPPTS complex was done through ion-exchange by adapting a literature procedure.<sup>27</sup> First, the Pd source and the TPPTS ligand (1 mmol), with a metal to ligand ratio of 1:5, were dissolved in deionized and degassed water under a flow of Ar (100 mL/min) and heated for 15 min at 353 K until the solution color became dark yellow indicating Pd/TPPTS complex formation. Subsequently, the solution was cooled to room temperature and the LDH was added (1 g) and the reaction mixture was stirred at room temperature for 24 h under a flow of Ar. Afterward the solid was separated by centrifugation, washed several times with water, and dried under a flow of Ar. The resulting materials were found to be air stable and were used without pretreatment in the catalytic reactions. The immobilized catalysts are denoted Pd/TPPTS/M1(II)M2(III)-(X)/ $\text{CO}_3$ , where M1 is the divalent metal cation, M2 the trivalent metal cation, and X is the anion.

The immobilization of the TPPTS ligand alone was done through ion-exchange by following a similar procedure in which the solution of ligand and the support were stirred for 24 h at room temperature. The resulting materials are denoted as *pseudo-heterogeneous* since just one of the two catalyst components of the complex was immobilized. The obtained pseudo-heterogeneous catalysts are denoted Pd+TPPTS/M1(II)M2(III)(X)/ $\text{CO}_3$ .

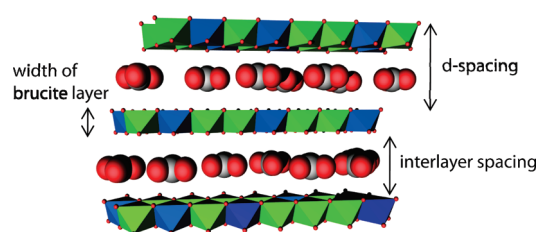
Post-synthesis of the Pd/TPPTS/ $\text{MgAl}-\text{Cl}/\text{CO}_3$  catalyst was done by reaction of the TPPTS/ $\text{MgAl}-\text{Cl}/\text{CO}_3$  material with a Pd source dissolved in water and stirred for 24 h at room temperature under an Ar flow.

**2. Catalyst Characterization.** XPS measurements were performed using a Specs GmbH setup. The excitation was done using a conventional dual anode X-ray source (Specs XR 50) using the Mg K $\alpha$  line (1253.6 eV). The sample consisted of a powder dispersed on two-sided adhesive tape. For the actual experiments, a pass energy of 30 eV (estimated resolution: 1.3 eV fwhm) was employed for the core levels and 50 eV for survey scans. The binding energies of Pd 3d and P 2p are referenced to the C1s peak of carbon at 284.8 eV.

Determination of the Pd and P content was done by inductively coupled plasma (ICP)-optical emission spectroscopy (OES) with a TJA Atomscan 16 machine.

X-ray powder diffraction (XRD) was performed using a Bruker-AXS D8 Advance powder X-ray diffractometer, equipped

### Scheme 1. Schematic Representation of a Layered Double Hydroxide with Interlayer Carbonate Anions



with automatic divergence slit, Vantec-1 detector and Cobalt  $K\alpha_{1,2}$  ( $\lambda = 1.79026 \text{ \AA}$ ) source.

The specific surface areas and pore volumes were determined by  $N_2$  sorption measurements using a Micromeritics ASAP 2400 instrument. Surface areas were calculated using the Brunauer–Emmett–Teller (BET) model.

FT-IR measurements were recorded on a Perkin-Elmer 2000 FTIR spectrometer with a data point resolution of  $4 \text{ cm}^{-1}$  with a DTGS detector with an accumulation of 16 scans per spectrum. The samples were diluted prior to measurement with KBr in a 5/95 mixture ratio.

Thermogravimetric analysis (TGA) was carried out on a Pyris TGA thermogravimetric analyzer from Perkin-Elmer with the sample held in ceramic pan in a continuous flow nitrogen atmosphere ( $10 \text{ mL/min}$ ). Samples were heated at a constant rate of  $5 \text{ K min}^{-1}$ .

**3. Catalyst Testing.** The standard conditions for the heterogeneous telomerization reactions are as follows. The reactions were performed in a 40 mL stainless steel Parr autoclave. The typical reaction composition consists of alcohol ( $3.8 \times 10^{-5} \text{ mol}$ ), and the catalyst (0.25 g) which were directly mixed inside the Parr autoclave and flushed three times with argon. The autoclave was cooled down to 233 K using an acetone-dry ice mixture. 1,3-Butadiene was directly condensed in the reactor, and the autoclave was heated to the reaction temperature of 363 K at which it was kept for 18 h. The starting point of the reactions was defined as the time at which the reaction temperature was reached. After the reaction, the reactor system was cooled to room temperature and flushed several times with argon. Similar reactions conditions were used for the homogeneous and pseudo-heterogeneous reactions, but metal loading and phosphine to metal ratios were adjusted accordingly. For the pseudo-heterogeneous reactions the loading of solid catalyst was kept at 0.25 g.

**4. Product Analysis.** Reaction products were filtered over a  $0.45 \text{ }\mu\text{m}$  filter. The reaction mixtures were analyzed using a GC 2010 system from Shimadzu with a CP-WAX 57CB ( $25 \text{ m} \times 0.2 \text{ mm} \times 0.2 \text{ }\mu\text{m}$ ) (internal calibration) and a GC-MS from Shimadzu with a CP-WAX 57CB column ( $25 \text{ m} \times 0.2 \text{ mm} \times 0.2 \text{ }\mu\text{m}$ ). For methanol and ethylene glycol (EG) telomers, authentic samples of the C8-telomers were prepared catalytically, purified by column chromatography and used for calibration.<sup>11</sup> Conversions and yields were calculated based on the alcohol.  $^1\text{H}$ - and  $^{13}\text{C}$  NMR APT spectra of the filtered and vacuum-dried reaction mixtures were recorded on a Varian AS400 or Varian Inova 300 instrument. Chemical shifts are reported in parts per million (ppm) relative to residual solvent signals (see Supporting Information).

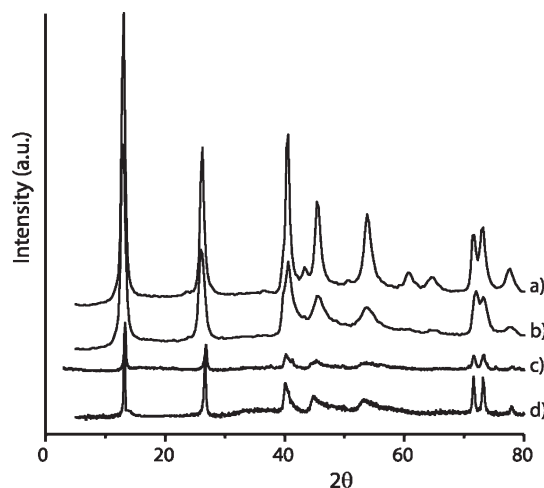


**Figure 1.** XRD patterns of the synthesized LDHs: (a) NiAl- $\text{NO}_3/\text{CO}_3$ , (b) NiAl- $\text{Cl}/\text{CO}_3$ , (c) MgAl- $\text{NO}_3/\text{CO}_3$ , and (d) MgAl- $\text{Cl}/\text{CO}_3$ .

## RESULTS AND DISCUSSION

**1. Catalyst Synthesis and Characterization.** To investigate the possibility of using layered double hydroxides as supports for the Pd/TPPTS telomerization system some well-known M(II)/M(III) combinations such as Mg/Al or Ni/Al were chosen with a fixed M(II)/M(III) ratio of 2. LDHs consist of positively charged brucite-like layers which are charge-balanced by intercalation of anions in the hydrated interlayer regions (Scheme 1). Ion exchange of these anions is possible, when the intercalated anions are chlorides or nitrates. Thus, hexagonal layered double hydroxide crystals were obtained having the general composition  $\text{Mg}_{1-x}\text{Al}_x(\text{OH})_2\text{Cl}_x \cdot n\text{H}_2\text{O}$  (MgAl- $\text{Cl}/\text{CO}_3$ ),  $\text{Mg}_{1-x}\text{Al}_x(\text{OH})_2(\text{NO}_3)_x \cdot n\text{H}_2\text{O}$  (MgAl- $\text{NO}_3/\text{CO}_3$ ),  $\text{Ni}_{1-x}\text{Al}_x(\text{OH})_2(\text{Cl})_x \cdot n\text{H}_2\text{O}$  (NiAl- $\text{Cl}/\text{CO}_3$ ) and  $\text{Ni}_{1-x}\text{Al}_x(\text{OH})_2(\text{NO}_3)_x \cdot n\text{H}_2\text{O}$  (NiAl- $\text{NO}_3/\text{CO}_3$ ) ( $x = 0.33$ ). The presence of carbonate anions in the layered double hydroxides, in addition to the chloride and nitrate anions, could not be avoided under our synthesis conditions, and they are therefore included in the abbreviation of the sample. In addition to the synthesized LDH materials, a commercial MgAl- $\text{CO}_3$  LDH (Mg/Al = 2) was used as a reference material.

X-ray powder diffraction (XRD) measurements of the as-synthesized materials show diffraction patterns characteristic of the corresponding LDHs (Figure 1). The lattice parameters derived from the diffraction data are presented in Table 1 and show values similar to the ones reported in literature and are typical for the corresponding type of LDH structures.<sup>29</sup> The parameter  $a$ , which corresponds to the cation–cation distance in the brucite-like layer of the LDH, has been calculated from the  $d$ -spacing of the (110) reflection and is 3.062 for the MgAl-LDHs and  $\sim 3.05$  for the NiAl-LDHs (Table 1). The parameter  $c$ , which is related to the thickness of the brucite-like layer and the interlayer space, has been calculated from the  $d$ -spacing of the (003) reflection.<sup>29</sup> The value of this parameter is directly influenced by the dimensions of the charge balancing anion, and for all the LDHs the obtained values are slightly higher than those expected for a LDH- $\text{CO}_3$ , indicating the presence of the nitrate and chloride anions in the interlayer space.<sup>29</sup>

The FT-IR spectra shown in Figure 2 further confirm the synthesis of the desired LDH structures. The broad band at  $3500 \text{ cm}^{-1}$  is attributed to the O–H stretching vibration of the

Table 1. Physical Properties of the Synthesized Materials

sample	lattice parameters				surface area BET (m <sup>2</sup> /g)	Pd (wt %)		P (wt %)
	<i>d</i> (003) Å	<i>d</i> (110) Å	<i>a</i> (Å)	<i>c</i> (Å)		ICP	ICP	
MgAl-Cl/CO <sub>3</sub>	7.794	1.531	3.062	23.383	50			
TPPTS/MgAl-Cl/CO <sub>3</sub>	15.270	1.531	3.062	45.810	38		0.93	
Pd/TPPTS/MgAl-Cl/CO <sub>3</sub>	16.760	1.531	3.062	50.300	40	0.65	0.90	
Pd/TPPTS/MgAl-Cl/CO <sub>3</sub> <sup>a</sup>	16.760	1.531	3.062	50.300	37	0.65	0.93	
MgAl-NO <sub>3</sub> /CO <sub>3</sub>	7.721	1.531	3.062	23.163	50			
Pd/TPPTS/MgAl-NO <sub>3</sub> /CO <sub>3</sub>	19.328	1.531	3.062	57.984	40	0.60	0.94	
MgAl-CO <sub>3</sub>	7.388	1.531	3.062	22.164	16			
NiAl-Cl/CO <sub>3</sub>	7.950	1.522	3.044	23.850	48			
Pd/TPPTS/NiAl-Cl/CO <sub>3</sub>	12.893	1.522	3.044	37.905	40	0.97	1.08	
NiAl-NO <sub>3</sub> /CO <sub>3</sub>	7.860	1.525	3.050	23.580	61			
Pd/TPPTS/NiAl-NO <sub>3</sub> /CO <sub>3</sub>	14.806	1.525	3.050	44.418	55	0.72	1.11	

<sup>a</sup> Catalyst obtained by post-synthesis.

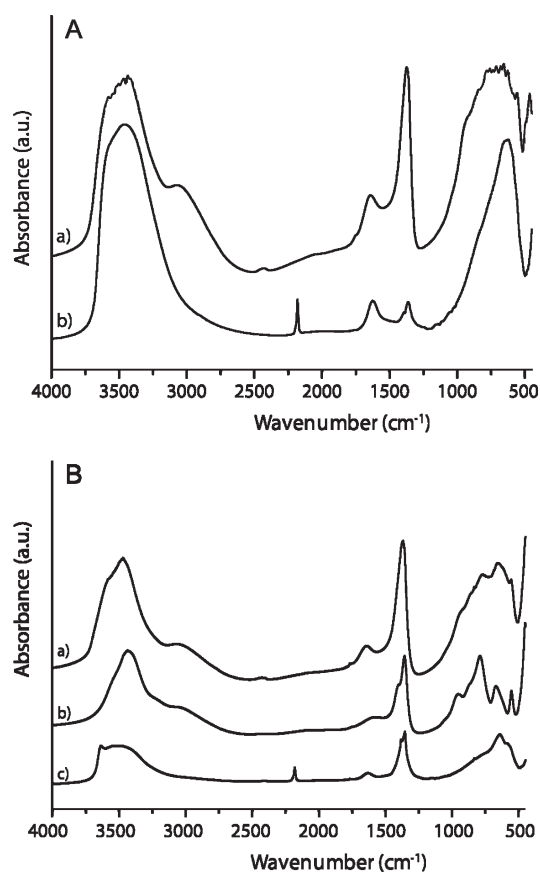


Figure 2. FT-IR spectra of the synthesized LDHs. (A) Synthesized LDH-Cl (a) MgAl-Cl/CO<sub>3</sub>; (b) NiAl-Cl/CO<sub>3</sub>; (B) Synthesized LDH-NO<sub>3</sub> (a) MgAl-NO<sub>3</sub>/CO<sub>3</sub>; (b) MgAl-NO<sub>3</sub>/CO<sub>3</sub>; and (c) NiAl-NO<sub>3</sub>/CO<sub>3</sub>.

hydrogen-bonded hydroxyl groups and of water molecules, which also give rise to a band at 1625 cm<sup>-1</sup> resulting from the bending vibration mode. LDH-CO<sub>3</sub> normally presents three characteristic bands at wavenumbers below 2000 cm<sup>-1</sup>, namely, at 1600 cm<sup>-1</sup>, 1360 cm<sup>-1</sup>, and 600–800 cm<sup>-1</sup> (Figure 2 B, a).<sup>29,30</sup> The band at 1360 cm<sup>-1</sup> is a vibration characteristic for the carbonate anion and was observed in all synthesized LDH materials, indicating that the carbonate is found together with

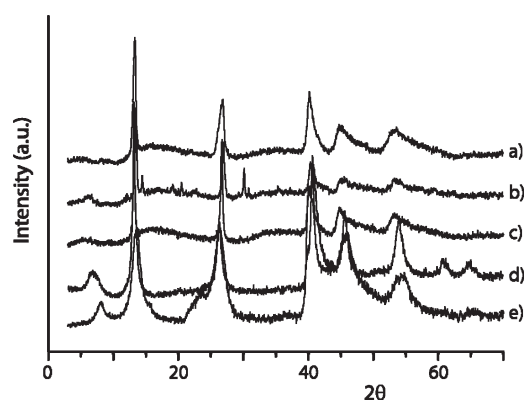
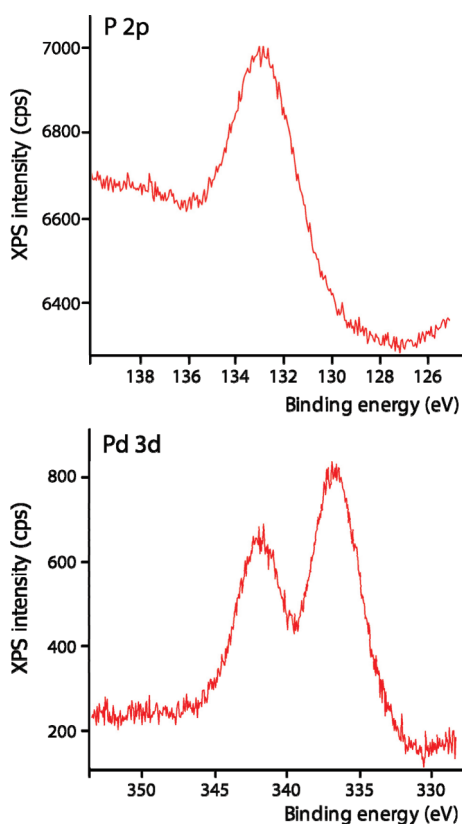


Figure 3. XRD patterns of the Pd/TPPTS/LDH materials: (a) Pd/TPPTS/MgAl-NO<sub>3</sub>/CO<sub>3</sub>, (b) Pd/TPPTS/MgAl-Cl/CO<sub>3</sub> (post-synthesis), (c) Pd/TPPTS/MgAl-Cl/CO<sub>3</sub>, (d) Pd/TPPTS/NiAl-NO<sub>3</sub>/CO<sub>3</sub>, and (e) Pd/TPPTS/NiAl-Cl/CO<sub>3</sub>.

the chloride or nitrate anions in the interlayers of the LDHs. For the NiAl-Cl/CO<sub>3</sub> sample a lower intensity of the carbonate band is observed, which points at a higher loading of chloride in the interlayer space than for the MgAl-Cl/CO<sub>3</sub> sample (Figure 2 A). For the MgAl-NO<sub>3</sub>/CO<sub>3</sub> and NiAl-NO<sub>3</sub>/CO<sub>3</sub> samples the presence of both nitrates and carbonates can be observed in the FT-IR spectra (Figure 2 B, spectra b and c). A band at 1381 cm<sup>-1</sup> which corresponds to the nitrate anion was observed in the FT-IR spectra of these material.<sup>27,29,30</sup> The obtained results, particularly those concerning the NiAl-NO<sub>3</sub>/CO<sub>3</sub> materials, confirm previous reports that indicate that incorporation of the nitrate anion into the final LDH structure is indeed possible despite the high affinity of the LDH structure for carbonates, even when they are used as coprecipitation reagents (as in this case from urea).<sup>27,29</sup>

Immobilization of the TPPTS ligand (pseudo-heterogeneous catalyst) or of a combination of Pd and TPPTS (heterogeneous catalyst) on the as synthesized supports was achieved by ion-exchange procedures. The XRD patterns of the catalysts immobilized on the LDH supports are presented in Figure 3. The reflection planes of the parent LDH materials are still observed in the samples, indicating that the immobilization procedure did not affect the stability and overall structure of the LDHs. By



**Figure 4.** Pd 3d and P 2p XPS spectra of the Pd/TPPTS/NiAl-Cl/CO<sub>3</sub> catalyst material.

incorporation of the TPPTS ligand or both Pd and TPPTS new reflection planes are observed at  $2\theta$  values of below  $10^\circ$ . This can be attributed to the incorporation of TPPTS or a Pd/TPPTS catalyst into the interlayer space of the LDH by ion-exchange, resulting in the formation of a new LDH phase.<sup>27,28,31,32</sup> The intensity of the reflection planes attributed to the phase containing (Pd/TPPTS) is much lower compared to the one of the parent NO<sub>3</sub>/CO<sub>3</sub> or Cl/CO<sub>3</sub> material, indicating that the ion-exchange process takes place only to a limited extent (Figure 3). For the NiAl-LDH samples (Figure 3 d and e), the intensity of these reflection planes is more pronounced compared to that of the MgAl samples (Figure 3 a, b and c) indicating a better incorporation of the Pd/TPPTS complex. This observation is in agreement with the loadings of Pd and P as determined by ICP analysis for these materials (Table 1). The loading of P (which indicates the amount of TPPTS) is 1 wt % for NiAl-LDH and 0.9% for MgAl-LDH. The diffraction planes at  $2\theta$  values around  $6^\circ$  obtained for the ion-exchanged supports corresponds to the (003) plane of the new LDH phase. The  $d$ -spacing of the (003) reflection increased from  $\sim 7$  Å for the parent to 12–19 Å for the synthesized materials (Figure 3 and Table 1) and corresponds to the interlayer space (gallery) plus the thickness of one brucite layer of the LDH structure. Taking in account a thickness of around 4.8 Å for the brucite layer, this means that the remaining gallery space is between 8 and 14 Å. As the size of one TPPTS ligand is around 12 Å, the observed increase in the interbrucite layer spacing suggests that it is the result of full intercalation of one TPPTS ligand or of partial intercalation of one ligand at the edges of the LDH structure. Previously, incorporation of related metal/TPPTS complexes into LDHs was assumed to involve the

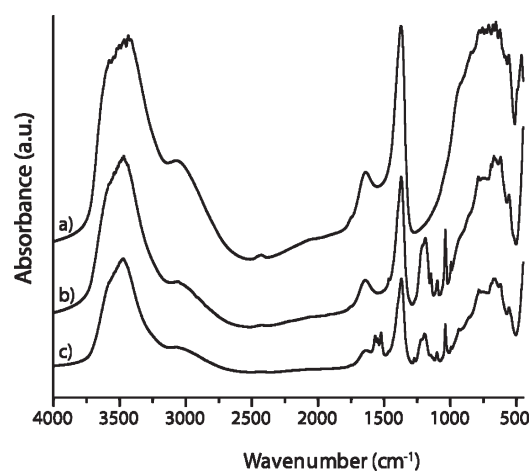


**Figure 5.** FT-IR spectra revealing the effect of the Pd/TPPTS incorporation into the LDH studied by FT-IR: (a) MgAl-Cl/CO<sub>3</sub>, (b) TPPTS/MgAl-Cl/CO<sub>3</sub>, and (c) Pd/TPPTS/MgAl-Cl/CO<sub>3</sub>.

binding of just one sulfonic acid group to the LDH structure, near the edge of the support.<sup>27,28</sup> Our results corroborate this view, as more extensive incorporation between the brucite sheets would have led to a higher intensity of those XRD patterns that correspond to the new LDH phase. Importantly, a direct consequence of this particular intercalation mode of the ligand is a high local concentration of potentially catalytically active species on the surface of the LDH.

The extent of immobilization of phosphine and palladium was determined by ICP, physisorption, and XPS measurements. The starting molar ratio used for the immobilization of TPPTS to Pd was 5:1 TPPTS/Pd. On the basis of the ICP results, the ratio of TPPTS/Pd in the final material is between 3.2 and 5. This is within the same range as previously reported, catalytically active Pd/TPPTS systems which commonly involve a TPPTS to Pd ratio of 3:1.<sup>2–7</sup> The incorporation of the TPPTS ligand or Pd/TPPTS complex is further confirmed by a decrease of the surface area of the resulting materials, as compared to the parent LDHs (see Table 1). The XPS analysis of the Pd/TPPTS/LDH catalysts indicated that Pd is mostly present in the Pd (0) oxidation state. This suggests that the excess of TPPTS ligand used in the synthesis is sufficient to reduce the Pd (II) precursor to Pd (0). For Pd/TPPTS/NiAl-Cl/CO<sub>3</sub>, for example, the binding energies of Pd 3d<sub>5/2</sub> and Pd 3d<sub>3/2</sub> are 336.3 eV and 341.5, respectively (Figure 4 a). This is a higher value than typically obtained for Pd (0) (335 eV),<sup>33</sup> which may indicate a partially cationic Pd species. The binding energy obtained for P 2p<sub>3/2</sub> is 132.3 eV, no phosphine oxide is detected by XPS (Figure 4 b); this is in agreement with previously reported data for TPPTS complexes.<sup>27,33</sup> The ratio of P to Pd obtained from the XPS measurement is 4.4; this is in close agreement with the one obtained from the ICP measurements (3.8) and further supports that most of the palladium and ligand are present at the surface of the LDH support.

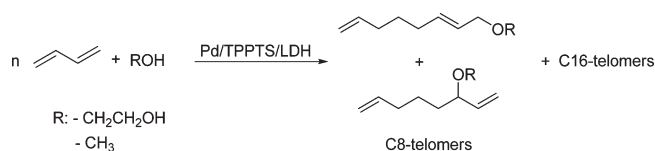
Finally, FT-IR measurements also show the presence of Pd/TPPTS on the LDH support after the ion-exchange process. The FT-IR spectra of the parent MgAl-Cl/CO<sub>3</sub>, TPPTS/MgAl-Cl/CO<sub>3</sub>, and Pd/TPPTS/MgAl-Cl/CO<sub>3</sub> materials are compared in Figure 5. The spectra show that bands corresponding to the TPPTS ligand appeared in the spectrum after complex immobilization. At the same time, the intensity of the carbonate bands

decreased, further indicating that ion exchange occurred. Characteristic infrared bands of TPPTS are the  $\nu_{\text{OSO}}$ ,  $\nu_{\text{SO}}$ , and  $\nu'_{\text{SO}}$  stretching vibrations which are generally found at 1196, 1040, and 628  $\text{cm}^{-1}$ , respectively.<sup>27,32</sup> In the FT-IR spectra of the Pd/TPPTS/LDH and TPPTS/LDH materials these bands appear to be shifted to lower frequencies (1185, 1035, and 615  $\text{cm}^{-1}$ ), which was previously attributed to the interaction of the sulfonic acid groups of the TPPTS with the LDH brucite layer after ion-exchange.<sup>32</sup> In addition, the vibration observed at 1600  $\text{cm}^{-1}$  can be assigned to the phenyl rings of the TPPTS ligand.

**2. Catalyst Activity Measurements.** The catalytic activity of the synthesized materials as well as of the unsupported Pd/TPPTS catalyst was evaluated in the telomerization of 1,3-butadiene with EG and methanol (Scheme 2). Ethylene glycol can be regarded as a model substrate for the more highly functionalized biomass-based polyols, whereas methanol telomerization was selected as this process is industrially employed for the production of 1-octene.<sup>4</sup> Note that Pd/TPPTS-catalyzed telomerization reactions are generally performed in the presence of both a solvent and a base activator.<sup>2–7</sup> Since our aim is to develop a catalyst capable of working under solvent-less conditions and without chemical additives, we tested both the homogeneous catalyst and our heterogeneous system under solvent- or base-free conditions. The homogeneous experiments that are included in the various tables are included for comparison with the (pseudo)-heterogeneous catalysts, and conditions, such as phosphine/Pd ratio and concentrations, therefore vary to allow comparison with the heterogeneous catalyst system.

**2.1. Telomerization Activity of the Homogeneous Catalysts.** The results of the catalytic tests performed with the homogeneous Pd/TPPTS complex without base or solvent are presented in Table 2. In the telomerization of 1,3-butadiene with EG the *mono*- and *di*-telomers (C8 telomers) were obtained as the major reaction products, mainly as the linear isomers (>95%) (Table 2, entries 1–4). Besides the two C8-telomer products, small amounts of higher telomers were also obtained with a combined selectivity of below 7%. On the basis of GC-MS and NMR analyses, it could be shown that these higher telomer products mainly consist of C16 *mono*-telomers. The NMR data (see Supporting Information) also shows that no branched isomers

**Scheme 2. Telomerization of 1,3-Butadiene with Methanol and Ethylene Glycol**



are formed; the higher telomers mainly consist of 6,1'-coupled C8 units, with only very minor amounts of the 8,1'-coupled isomer and none of the 6,3'-coupled one (see Supporting Information). The various isomers were not further quantified; however, because of the low yield of some these products. The fact that such products were not previously reported in the telomerization of 1,3-butadiene with EG with a Pd/TPPTS catalyst may be due to the different reaction conditions that are normally employed, that is, the use of additional bases and solvents. Interestingly, higher telomer products were reported in the telomerization of 1,3-butadiene with alcohols when a cationic Pd allyl complex was used as homogeneous catalyst (*vide infra*).<sup>34–36</sup>

Since the active complex is formed in situ, the Pd source is expected to have a strong influence on the telomerization activity. Indeed, a higher telomerization activity was obtained (86% conversion of EG) using a Pd(0) metal source (Pd(dba)<sub>2</sub>) compared to the cationic Pd(II) metal precursor (56% conversion) (Table 2, entries 1–2). The influence of an LDH on the activity of the Pd/TPPTS complex was tested by adding it to the reaction mixture together with the homogeneous catalyst (Table 2, entries 3–4). The results show that the telomerization activity of Pd/TPPTS could be enhanced by the addition of the LDH. Conversion of EG increased from 56% to 76% when MgAl-Cl/CO<sub>3</sub> was added and to 83% with MgAl-CO<sub>3</sub>. The main reaction products were still the *mono*- and the *di*-telomers, but a slight increase in selectivity for the higher telomers was observed from 7% to around 10–11% after LDH addition. Furthermore, an increase in TON was observed from 573 to 751 and 827 for MgAl-Cl/CO<sub>3</sub> and MgAl-CO<sub>3</sub>, respectively (Table 2 entries 3 and 4). The enhanced catalytic activity observed by LDH addition can most probably be attributed to its basic properties,<sup>37–39</sup> as bases are well known to promote the activity of the telomerization catalysts, in particular for Pd/TPPTS-catalyzed reactions.<sup>2</sup> Therefore, the LDH can be used as an environmentally friendly alternative to the homogeneous alkaline salts, as the solid base can be easily recovered and reused. The support itself exhibited no telomerization activity as no conversion was observed with either a MgAl or NiAl-based LDH alone. The LDH material recovered from the previous catalytic experiment (i.e., Pd/TPPTS plus added LDH) showed a very small conversion of 1–2% after 24 h of reaction, however, indicating that some adsorption of the Pd/TPPTS complex may occur during the telomerization process.

Telomerization of 1,3-butadiene with methanol over Pd/TPPTS was also investigated under these solvent and base-free conditions. Very good conversions were obtained after just 4 h of reaction (Table 2, entries 5–6). The high activity is further evidenced by the high TONs of 1086 and 1207. The improved telomerization activity of methanol compared to EG may be

**Table 2. Telomerization Activity of the Homogeneous Pd/TPPTS Catalyst<sup>a</sup>**

entry	substrate	Pd source	additive	time (h)	conv. (%)	sel. <sub>mono-C8</sub> (%)	sel. <sub>di-C8</sub> (%)	sel. <sub>higher</sub> (%)	TON
1	EG	Pd(dba) <sub>2</sub>		18	86	66	27	7	955
2		Pd(acac) <sub>2</sub>		18	56	77	17	6	573
3		Pd(acac) <sub>2</sub>	MgAl-Cl/CO <sub>3</sub>	18	76	73	15	10	751
4		Pd(acac) <sub>2</sub>	MgAl-CO <sub>3</sub>	16	83	69	17	11	827
5	MeOH	Pd(acac) <sub>2</sub>		4	60	89		10	1207
6		Pd(dba) <sub>2</sub>		4	54	90		9	1086

<sup>a</sup> Reaction conditions: 0.26 mmol TPPTS, 0.08 mmol Pd, 363 K, 1,3-Bu/alcohol ratio of 2:1. Substrate concentrations: 0.07 mol EG or 0.16 mol MeOH.

**Table 3. Telomerization of 1,3-Butadiene with Alcohols with a Pseudo-Heterogeneous LDH Based Catalyst<sup>a</sup>**

entry	substrate	catalyst	Pd source	conv. (%)	sel. <sub>mono-C8</sub> (%)	sel. <sub>di-C8</sub> (%)	sel. <sub>higher</sub> (%)	TON
1 <sup>b</sup>	EG	Pd/TPPTS	Pd(dba) <sub>2</sub>	54	86	10	2	874
2		Pd+TPPTS/MgAl-Cl/CO <sub>3</sub>	Pd(acac) <sub>2</sub>	37	39	19	42	660
3		Pd+TPPTS/NiAl-NO <sub>3</sub> /CO <sub>3</sub>	Pd(dba) <sub>2</sub>	34	35	11	48	536
4 <sup>c</sup>	MeOH	Pd+TPPTS/NiAl-NO <sub>3</sub> /CO <sub>3</sub>	Pd(dba) <sub>2</sub>	20	30		65	389

<sup>a</sup> Reaction conditions: 0.250 g TPPTS/LDH, 0.08 mmol Pd, 0.08 mmol TPPTS, 363 K, 1,3-Bu/EG of 2:1. <sup>b</sup> 0.12 mol EG, 18 h. <sup>c</sup> 0.16 mol MeOH, 90 min.

caused by the fact that 1,3-butadiene dissolves better in methanol than in EG resulting in a more homogeneous reaction mixture. This then leads to a better access of the reactant molecules to the catalytically active species.<sup>11</sup> As in the case of telomerization of 1,3-butadiene with EG, the *mono*-C8 telomer was obtained as the major product with a selectivity close to 90%. The formation of some higher telomers was observed as a byproduct with selectivities of up to 10%.

**2.2. Telomerization Activity of the Pseudo-Heterogeneous Catalysts.** Most of the reports concerning the development of heterogeneous telomerization catalysts refer to either metal or ligand immobilization but not to the combination of both.<sup>19–23</sup> The use of an LDH support offers the possibility to investigate the effect of the immobilization of the catalyst components (i.e., palladium or ligand) and of the preformed complex itself on the telomerization activity, selectivity, and catalyst stability. In Table 3 the results are presented of the telomerization of 1,3-butadiene with the pseudo-heterogeneous catalysts obtained by the immobilization of the ligand or metal and the separate addition of the other catalyst component to the reaction mixture (see the Experimental Section). Good telomerization activities were obtained when TPPTS/LDH was used as a solid and Pd was added separately to the reaction (Table 3, entries 2–3). The results were compared to those obtained with a homogeneous Pd/TPPTS reaction with a Pd to TPPTS molar ratio similar to the pseudo-heterogeneous catalyst (Table 3, entry 1). The conversion of EG decreased from 54% to 34–37% with the pseudo-heterogeneous catalyst, although TONs of over 500 were still obtained. These TONs are comparable to those obtained in the telomerization of methanol with a Pd/TPPTS system immobilized on KF/Al<sub>2</sub>O<sub>3</sub> (TONs of up to 440 h<sup>-1</sup>), for instance.<sup>20</sup> It has to be noted, however, that direct comparison is difficult given the different temperature and ratio of reactants employed. A more interesting change was observed in the product distribution. The main reaction products with the homogeneous Pd/TPPTS complex were the typical C8-telomers, that is, the *mono*- and *di*-telomer of EG. The use of a pseudo-heterogeneous catalyst with just the ligand immobilized, on the other hand, mainly resulted in the formation of higher telomers; in particular C16 *mono*-telomers (found with >90% yield in the higher telomers mixture) were now obtained as main reaction products (Table 3, entries 2–3). Product analysis by <sup>13</sup>C NMR APT measurements clearly showed that these higher telomers contain a strong tertiary carbon signal. This indicates that the higher telomers are formed via a C–C coupling reaction between a secondary and a primary carbon atom resulting in a branched structure (see Supporting Information). The mechanistic implications of these observations are discussed further below. Immobilization of Pd alone with or without separate addition of the TPPTS ligand was also investigated (data not shown). No telomerization activity was observed in the absence

of the phosphine. When the ligand was added homogeneously, the telomerization activity resembled that of the homogeneous catalyst and extensive leaching of Pd, indicated by the color change of the solution, occurred. The telomerization of 1,3-butadiene with methanol over pseudo-heterogeneous catalysts such as TPPTS/NiAl-NO<sub>3</sub>/CO<sub>3</sub> and Pd(dba)<sub>2</sub> yielded, as in the case of EG, mainly higher telomers with 65% selectivity (C16-telomer with 33% selectivity) (Table 3, entry 4) and a TON of 389 after just 90 min of reaction.

**2.3. Telomerization Activity of the Heterogeneous Catalysts.** Finally, the catalytic activity of immobilized Pd/TPPTS catalysts was tested in the telomerization of 1,3-butadiene. As expected, the catalytic activity and product distribution were influenced by the immobilization route, the type of LDH support and the alcohol substrate (Table 4). All heterogeneous Pd/TPPTS/LDH catalysts gave a lower conversion of EG compared to the homogeneous and pseudo-heterogeneous catalysts (Tables 2 and 3). This can be attributed to the low palladium loading of the Pd/TPPTS/LDH materials, as exemplified by the ICP and XPS results. Indeed, the amount of Pd in the heterogeneous catalysts is almost 6 times lower than the amount of Pd used in standard homogeneous reactions (see Table 2). Using a similar concentration of Pd/TPPTS in the homogeneous reaction as in the supported samples the conversion dropped to 10% after 18 h of reaction (Table 4, entry 1). The TON was similar to the one obtained with a higher catalyst concentration, however. The TON can therefore be conveniently used to assess the activity of the immobilized catalysts. By comparing the TONs (determined by the number of moles of metal) obtained for the immobilized Pd/TPPTS catalysts with the homogeneous system similar values were obtained indicating that the activity of the catalyst is preserved during immobilization. The observed TONs are of the same order of magnitude as were for instance reported for Pd/TPPTS/KF/Al<sub>2</sub>O<sub>3</sub>.<sup>20</sup> The observed TONs are of course lower than those obtained with other telomerization catalysts. For homogeneous methanol telomerization catalysts, high TONs of up to 37000<sup>4</sup> or >250000<sup>8</sup> have for instance been reported. It should be noted, however, that for a fair comparison, the activity of the heterogeneous system should be directly compared to its homogeneous analogue (Table 4, entry 1). The data shows that no activity is lost upon immobilization. The observed TONs are the direct consequence of the rather low loadings of catalyst on the LDHs, which could be improved for further catalyst development.

Pd/TPPTS immobilized on MgAl-LDHs by direct synthesis (Table 4, entries 2 and 5) present conversions of EG below 5%, with a high selectivity for the *mono*-telomer of above 80%. The choice of LDH support clearly affects both product distribution and activity. The TON of the Pd/TPPTS/MgAl-Cl/CO<sub>3</sub> catalyst is 233, whereas for Pd/TPPTS/MgAl-NO<sub>3</sub>/CO<sub>3</sub> a TON of just 92 is obtained. Also, the selectivity of 16% for the higher

Table 4. Telomerization of 1,3-Butadiene with Alcohols with the Heterogenized Pd/TPPTS/LDH Catalysts<sup>a</sup>

entry	substrate	catalyst	conv. (%)	sel. <sub>mono-C8</sub> (%)	sel. <sub>di-C8</sub> (%)	sel. <sub>higher</sub> (%)	TON
1 <sup>b</sup>	EG	Pd/TPPTS	10	80	17	3	411
2		Pd/TPPTS/MgAl-Cl/CO <sub>3</sub>	5	82	2	16	233
3 <sup>c</sup>		Pd/TPPTS/MgAl-Cl/CO <sub>3</sub>	16	61	5	34	768
4		Pd/TPPTS/NiAl-Cl/CO <sub>3</sub>	4	77	7	12	120
5		Pd/TPPTS/MgAl-NO <sub>3</sub> /CO <sub>3</sub>	2	89	0	10	92
6		Pd/TPPTS/NiAl-NO <sub>3</sub> /CO <sub>3</sub>	5	44	10	43	230
7 <sup>d</sup>		Pd/TPPTS/NiAl-NO <sub>3</sub> /CO <sub>3</sub>	4	46	21	19	370
8 <sup>e</sup>		Pd/TPPTS/NiAl-NO <sub>3</sub> /CO <sub>3</sub>	7	28	33	30	616
9 <sup>f</sup>	MeOH	Pd/TPPTS/MgAl-Cl/CO <sub>3</sub>	51	18		77	1333
10 <sup>g</sup>		Pd/TPPTS/NiAl-NO <sub>3</sub> /CO <sub>3</sub>	29	27		66	1484
11 <sup>h</sup>		Pd/TPPTS/NiAl-NO <sub>3</sub> /CO <sub>3</sub>	13	18		72	1121
12 <sup>h</sup>		Pd/TPPTS/NiAl-Cl/CO <sub>3</sub>	16	19		70	1016

<sup>a</sup> Reaction conditions 0.250 g of catalyst, 363 K, 18 h, 1,3-Bu/alcohol of 2:1, 0.07 mol alcohol. <sup>b</sup> 0.02 mmol Pd(acac)<sub>2</sub>, 0.06 mmol TPPTS. <sup>c</sup> Catalyst prepared by post-synthesis. <sup>d</sup> 0.120 g catalyst, 16 h, 10 mL THF. <sup>e</sup> 0.12 mol EG. <sup>f</sup> 0.09 mol MeOH, 0.6 g catalyst and 16 h. <sup>g</sup> 0.09 mol MeOH and 4 h. <sup>h</sup> 0.16 mol MeOH, 4 h.

telomers increased for Pd/TPPTS/MgAl-Cl/CO<sub>3</sub> (Table 4, entry 2), as compared to the nitrate-based LDH support (10%) (Table 4, entry 5).

The Pd/TPPTS/MgAl-Cl/CO<sub>3</sub> catalyst obtained by post-synthesis (i.e., sequential immobilization of ligand followed by palladium) presented the highest telomerization activity of the series studied. The conversion of EG was 16% (TON 768), and the selectivity for the *mono*-telomer was just 62%, where the higher telomers were obtained with 34% selectivity (Table 4, entry 3). The post-synthesis method, as indicated by the XRD and FT-IR data, led to a higher amount of immobilized complex which in turn accounts for the higher catalytic activity. The Pd/TPPTS/NiAl-LDHs presented EG conversions similar to the Pd/TPPTS/MgAl-LDH materials, but some differences were observed in the product distribution, since a higher selectivity was observed for the higher telomers for some of the NiAl-LDH-based catalysts. Particularly, Pd/TPPTS/NiAl-NO<sub>3</sub>/CO<sub>3</sub> showed 43% selectivity for the higher telomers (Table 4, entry 6) with a TON of 230. The Pd/TPPTS/NiAl-Cl/CO<sub>3</sub> had a selectivity of just 12% for higher telomers with a TON of 120 under similar reaction conditions (Table 4, entry 5). The use of a solvent such as tetrahydrofuran (THF) reduced the selectivity toward higher telomers (Table 4, entry 7) from 43% to 19%, but the TON increased to 370. Given the similar alcohol conversion, this increase is explained by the fact that the formation of *mono*-C8 and of higher telomers account for a TON of 1, whereas the formation of *di*-C8 telomers accounts for a TON of 2. Decreasing the catalyst loading has an interesting influence on the product distribution (Table 4, entry 8). In this case, the *di*-telomer was obtained as the main reaction product with 33% selectivity, with selectivities for the *mono*-telomer and higher telomers of 28% and 30%, respectively.

Higher conversions were obtained in the telomerization of 1,3-butadiene with methanol over the Pd/TPPTS/LDH catalysts than with EG (Table 4, entries 9–12). Once again the higher solubility of 1,3-butadiene in methanol may allow a better accessibility of the reactants to the catalytically active species thus determining the higher activity. TONs of over a 1000 were obtained after 4 h of reaction, comparable to the TONs obtained with the homogeneous catalyst. As previously observed for the

pseudo-heterogeneous catalysts, the higher telomers of methanol were also here obtained as the main reaction products. With an increased reaction time (16 h instead of 4 h) and catalyst loading, a methanol conversion of 51% and selectivity for the C8 telomer of 18% and 77% for higher telomers could be obtained (Table 4, entry 9).

**2.4. Heterogeneity Tests and Reuse of the Pd/TPPTS/LDH Catalysts.** The heterogeneity and reusability of the immobilized telomerization catalysts were investigated for both the heterogeneous and the pseudo-heterogeneous catalysts. The recovery and reuse of the best performing system Pd/TPPTS/MgAl-Cl/CO<sub>3</sub> is presented in Table 5. The catalyst was recovered and reused for two reaction cycles. In the second run a decrease of the conversion was observed from 16% to 10%, but the selectivity remained almost the same (Table 5, entries 1–2). The heterogeneity of this system was investigated by performing a hot filtration test in which the catalyst was removed after 2 h of reaction and the filtrate was left to run under reaction conditions for another 16 h (Table 5, entries 3–4). Hardly any activity was seen after filtration, with only a 1% increase in conversion after 16 h. This small increase can probably be attributed to small particles that went through the filter. This is further substantiated by the observed increase in selectivity for higher telomers after filtration (16% vs no higher telomers before filtration), as the homogeneous catalyst is not promoting higher telomer formation. Our previous results show that this reaction is promoted by the LDH, which indicates that some of the support material must still be present after filtration (Table 5).

FT-IR analysis of the spent catalyst indicated that a carbonaceous deposit is formed during the catalytic process, most probably oligomerized butadiene species (Figure 6). New bands appear at 3073, 2915, and 2859 cm<sup>-1</sup> which correspond to aromatic [CH], alkyl  $\nu_s$  [CH<sub>3</sub>], and  $\nu_{as}$  [CH<sub>2</sub>] vibrations, respectively. Also, an increase in intensity of the 1650 cm<sup>-1</sup> band was observed, which may be the result of coke formation, but might also correspond to adsorbed water molecules. A band at 1440 cm<sup>-1</sup> corresponding to [CH<sub>3</sub>] asymmetrical bending was also observed.<sup>40</sup>

In addition, the recovery and reuse of the pseudo-heterogeneous TPPST/LDH catalyst was attempted (Table 6). Without



**Table 5. Recovery and Re-Use of the PdTPPTS/MgAl-Cl/CO<sub>3</sub> Catalyst in the Telomerization of 1,3-Butadiene with Ethylene Glycol<sup>a</sup>**

catalyst		time (h)	conv. (%)	sel. <sub>mono-C8</sub> (%)	sel. <sub>di-C8</sub> (%)	sel. <sub>higher</sub> (%)
PdTPPTS/MgAl-Cl/CO <sub>3</sub>	first run	18	16	61	5	34
PdTPPTS/MgAl-Cl/CO <sub>3</sub>	second run	18	10	65	4	30
PdTPPTS/MgAl-Cl/CO <sub>3</sub>		2	1	93		
PdTPPTS/MgAl-Cl/CO <sub>3</sub> <sup>b</sup>	hot filtration	16	2	83	1	16

<sup>a</sup> Reaction conditions: 0.250 g of catalyst, 0.06 mol EG, 363 K, 1,3-Bu/EG of 2:1. <sup>b</sup> The catalyst was filtered from the hot solution and a new amount of 1,3-butadiene was added.

**Table 6. Recovery and Re-Use of the Pseudo-Heterogeneous Catalyst in the Telomerization of 1,3-Butadiene with Ethylene Glycol<sup>a</sup>**

catalyst	Pd added	conv. (%)	sel. <sub>mono-C8</sub> (%)	sel. <sub>di-C8</sub> (%)	sel. <sub>higher</sub> (%)
TPPTS/NiAl-NO <sub>3</sub> /CO <sub>3</sub>	yes	34	35	11	48
run-2	no	2	60	16	22
run-3	yes	17	37	16	38

<sup>a</sup> Reaction conditions: 0.250 g of catalyst, 0.12 mol EG, 363 K, 18 h, 0.08 mmol Pd(dba)<sub>2</sub>, 1,3-Bu/EG 2:1.

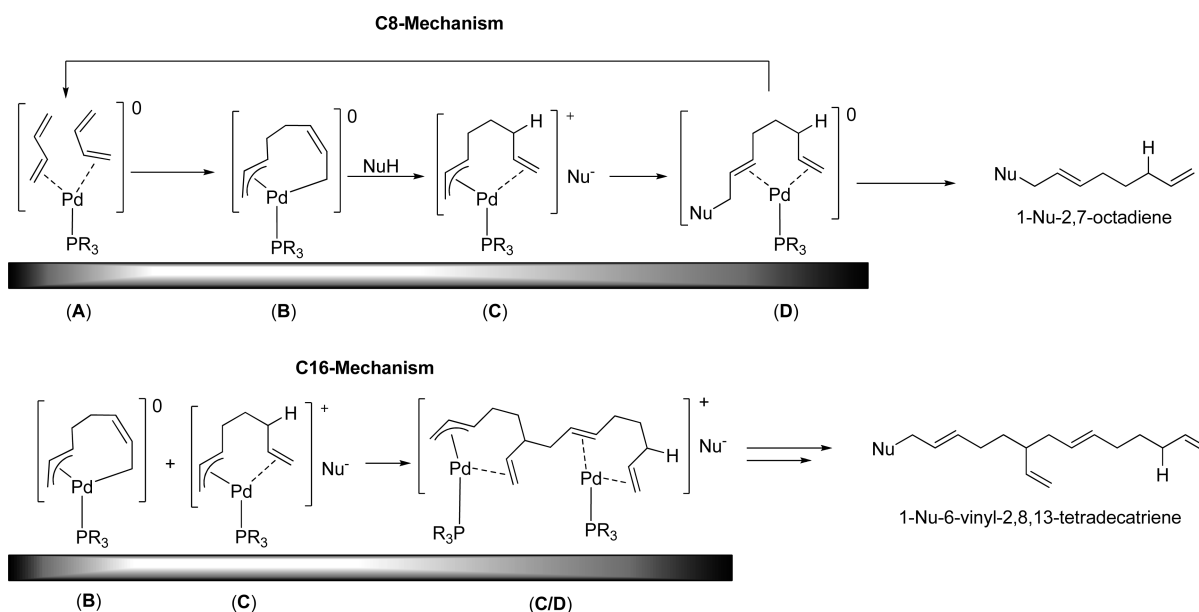
the addition of a fresh amount of Pd in the second run the catalytic activity dropped sharply to around 4–5%, while the selectivity was preserved (Table 6, entries 1–2). This indicates that some of the Pd initially present remained bound by the phosphine ligand after reaction, but this amount must be very small. Addition of a fresh amount of Pd precursor, however, restores some of the activity as well as the selectivity, and values closer to those of the first run are obtained. Deposits of black “coke”-like material are observed after each run, and this may contribute to the loss of telomerization activity in time (Table 6, entry 3).

### 3. Solid Catalyst C8/C16-Product Formation Mechanism.

The formation of higher telomers has previously been reported for the telomerization of 1,3-butadiene with methanol by cationic  $\eta^3$ -allylpalladium complexes, which are stabilized by mono- or bidentate ligands.<sup>34–36</sup> With these catalysts, C16-telomers of various alcohols were obtained with selectivities higher than or similar to those obtained for the C8-telomers. The formation of these higher telomers was proposed to occur via condensation of C8-units, since almost all of the higher telomers contained even numbers of butadiene monomers.<sup>34</sup> Furthermore, the immobilization of these cationic  $\eta^3$ -allylpalladium(II) complexes on ion-exchange resins and their use in the telomerization of 1,3-butadiene with methanol resulted in formation of C16-telomers, albeit with a selectivity lower than that of the homogeneous catalyst.<sup>36</sup> Tkatchenko et al. proposed a possible mechanism for the formation of these higher telomers by postulating the involvement of methoxide-bridged/supported bimetallic Pd-complexes.<sup>35</sup> These tentative species are similar to the acetate-bridged palladium dimers in the dipalladium-bisallyl mechanism demonstrated by Keim et al. for the telomerization of phenol or acetic acid, but no direct evidence for the methoxide-bridged/supported bimetallic Pd-complexes was presented. One could also imagine that higher telomer formation would be the result of telomerization of initially formed 1,3,7-octatriene C8 units. The lack of telomers with odd numbered butadiene units, (the absence of the C12 telomer as main product in particular) and the NMR data that we have obtained point against this route, however. We prefer an alternative explanation which is based on the classical telomerization mechanism proposed by Jolly et al.<sup>41,42</sup> The increased selectivity for higher telomers containing

even numbers of butadiene units may thus be explained by C–C bond formation between two distinct catalytic intermediates. The proposed mechanistic routes for the synthesis of both C8- and C16-telomers on the solid catalysts are presented in Scheme 3. The classical C8-mechanism shows that the intermediate [Pd(1,2,3,8- $\eta^4$ -2,6-octadien-1,8-diyl)(L)] (B) is mainly protonated by the substrate to give [Pd(1,2,3,7,8- $\eta^5$ -2,7-octadien-1-yl)(L)]<sup>+</sup> (C) during catalysis. Complex C, in turn, is attacked by the conjugate base of the substrate to give product complex [Pd(2,3,7,8- $\eta^4$ -1-alkoxy-2,7-octadiene)(L)] (D). Subsequently, the ligated telomer is displaced by butadiene resulting in species A, thereby completing the catalytic cycle. It should be pointed out that the C8 ligand of species B is bonded both as a  $\pi$ -allylic as well as a  $\sigma$ -allylic ligand and can accordingly act as both an electrophile and a nucleophile/base.<sup>43</sup> The nucleophilic nature of  $\eta^1$ -allyl palladium species is well documented.<sup>44</sup> In addition, Kiji et al. have demonstrated the nucleophilic nature of B in the telomerization of butadiene in the presence of an electrophile, benzaldehyde, obtaining the expected pyran product.<sup>45</sup> Indeed, when the  $\sigma$ -allylic fragment in B is sufficiently nucleophilic, it is plausible that a direct reaction between the 6-position of species B and the 1-position of C can give rise to the bimetallic complex C/D resulting in a C16-telomer with a branched carbon chain (Scheme 3). The <sup>13</sup>C NMR APT experiments, with the tertiary carbon signal resulting from electrophilic attack of C at the 6-position of the  $\eta^3, \eta^1$ -ligand, further corroborate this. In case of homogeneously catalyzed reactions both the generally low catalyst concentrations as well as the electrostatic attraction between C and Nu<sup>−</sup> will favor product formation via addition of the nucleophile over chain transfer via the reaction between B and C. However, in case of the heterogeneous TPPTS/LDH catalysts, the active species are localized on the external surface and edges of the solid, resulting in a high local catalyst concentration. This enhances the probability of reactions between active complexes. In addition, the polycationic nature of the LDH may also act by trapping the nucleophile on the surface so that coupling reactions get a chance to occur before product formation, thus enhancing higher telomer production. The (limited) formation of higher telomers under homogeneous conditions in the absence of a base (vide supra) can thus also be understood,

**Scheme 3. Telomerization Mechanism of 1,3-Butadiene with Pd/Phosphine Catalysts: (a) Classical Mechanism for C8 Telomer Formation, (b) Chain Transfer on LDH Support Leading to Higher (C16+) Telomers<sup>a</sup>**



<sup>a</sup> Formation of the branched isomers is not observed.

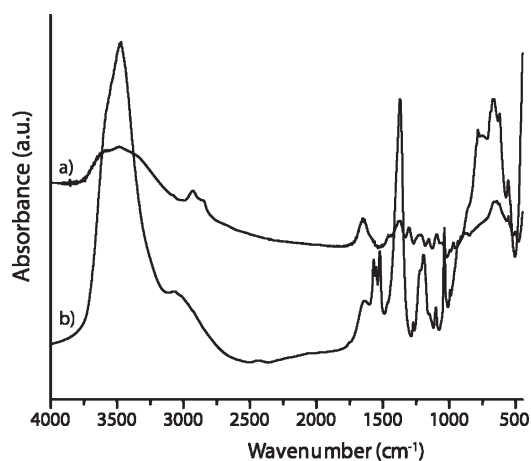


**Figure 6.** FT-IR spectra of (a) the spent Pd/TPPTS/MgAl-Cl/CO<sub>3</sub> (post synthesis) catalyst and (b) the fresh Pd/TPPTS/MgAl-Cl/CO<sub>3</sub> (post synthesis) catalyst.

given our observation of the rather sluggish reactivity of intermediate C with the methoxide nucleophile, in the case of TPPTS.<sup>13</sup> Indeed both the catalytic results as well as the fact that mainly branched higher telomers are observed (Scheme 3) provide strong evidence for the proposed reaction pathway.

## CONCLUSIONS

The immobilization of a Pd/TPPTS complex or the TPPTS ligand on layered double hydroxides (LDH) by ion-exchange was investigated. The catalytic activity of the thus obtained heterogeneous catalysts was tested in the telomerization of 1,3-butadiene with biomass-based alcohols, such as EG and methanol. The LDH support was found to have a positive effect on the activity of the Pd/TPPTS complex. Remarkably, the immobilization of the ligand or the complex leads to a dramatic change in product distribution. By

using the LDH-based pseudo-heterogeneous and heterogeneous catalysts higher telomers of the alcohols, identified to consist of mostly C16 *mono*-telomers, were obtained with high selectivities. This effect of the LDH on the product distribution was attributed to the capacity of the support to trap the catalytic intermediates on the surface. The high local catalyst concentration in turn is proposed to result in C–C bond formation reactions between distinct catalytic intermediates. The amount of complex immobilized on the support was influenced by the preparation route and the type of the LDH. Ni–Al based LDH seems to be a better support for the Pd/TPPTS complex, as suggested by the XRD and ICP measurements, but the telomerization activities were found to be similar. The highest telomerization activity was obtained with a PdTPPTS/MgAl-Cl/CO<sub>3</sub> catalyst obtained by the post-synthesis method. The properties of the alcohol also strongly influenced the telomerization activity as considerably higher conversions were obtained for telomerization of 1,3-butadiene with methanol. The recovery and reuse of the telomerization catalysts was investigated and proved possible.

## ASSOCIATED CONTENT

**S Supporting Information.** Identification of the reaction products (GC-MS data) and the <sup>1</sup>H and <sup>13</sup>C NMR spectra of the telomerization reaction mixtures. This material is available free of charge via the Internet at <http://pubs.acs.org>.

## AUTHOR INFORMATION

### Corresponding Author

\*E-mail: [b.m.weckhuysen@uu.nl](mailto:b.m.weckhuysen@uu.nl).

## ACKNOWLEDGMENT

The authors kindly thank ACTS-ASPECT for financial support.

## REFERENCES

- (1) Smutny, E. J. *J. Am. Chem. Soc.* **1967**, *89*, 6793–6794.
- (2) Behr, A.; Becker, M.; Beckmann, T.; Johnen, L.; Leschinski, J.; Reyer, S. *Angew. Chem., Int. Ed.* **2009**, *48*, 3598–3614.
- (3) Clement, N. D.; Routaboul, L.; Grotevendt, A.; Jackstell, R.; Beller, M. *Chem.—Eur. J.* **2008**, *14*, 7408–7420.
- (4) Tschan, M. J.-L.; Garcia-Suarez, E. J.; Freixa, Z.; Launay, H.; Hagen, H.; Benet-Buchholz, J.; van Leeuwen, P. W. N. M. *J. Am. Chem. Soc.* **2010**, *132*, 6463–6473.
- (5) Mesnager, J.; Quettier, C.; Lambin, A.; Rataboul, F.; Pinel, C. *ChemSusChem* **2009**, *2*, 1125–1129.
- (6) Mesnager, J.; Quettier, C.; Lambin, A.; Rataboul, F.; Perrard, A.; Pinel, C. *Green Chem.* **2010**, *12*, 475–482.
- (7) Bouquillon, S.; Muzart, J.; Pinel, C.; Rataboul, F. *Top. Curr. Chem.* **2010**, *295*, 93–119.
- (8) Grotevendt, A.; Jackstell, R.; Michalik, D.; Gomez, M.; Beller, M. *ChemSusChem* **2009**, *2*, 63–70.
- (9) Palkovits, R.; Nieddu, I.; Kruithof, C. A.; Klein Gebbink, R. J. M.; Weckhuysen, B. M. *Chem.—Eur. J.* **2008**, *14*, 8995–9005.
- (10) Palkovits, R.; Nieddu, I.; Klein Gebbink, R. J. M.; Weckhuysen, B. M. *ChemSusChem* **2008**, *1*, 193–196.
- (11) Palkovits, R.; Parvulescu, A. N.; Hausoul, P. J. C.; Kruithof, C. A.; Klein Gebbink, R. J. M.; Weckhuysen, B. M. *Green Chem.* **2009**, *11*, 1155–1160.
- (12) Hausoul, P. J. C.; Bruijninx, P. C. A.; Klein Gebbink, R. J. M.; Weckhuysen, B. M. *ChemSusChem* **2009**, *2*, 855–858.
- (13) Hausoul, P. J. C.; Parvulescu, A. N.; Lutz, M.; Spek, A. L.; Bruijninx, P. C. A.; Weckhuysen, B. M.; Klein Gebbink, R. J. M. *Angew. Chem., Int. Ed.* **2010**, *122*, 8144–8147.
- (14) Tokitoh, Y.; Higashi, T.; Hino, K.; Murasawa, M.; Yoshimura, N. (Kuraray), U.S. Patent US 5118885, 1992.
- (15) Briggs, J.; Patton, J.; Vermaire-Louw, S.; Margl, P.; Hagen, H.; Beigzadeh, D. (Dow Global Technologies Inc.), Patent WO 2010019360, 2010.
- (16) Pennequin, I.; Meyer, J.; Suisse, I.; Mortreux, A. *J. Mol. Catal. A: Chem.* **1997**, *120*, 139–142.
- (17) Behr, A.; Urschery, M. *Adv. Synth. Catal.* **2003**, *345*, 1242–1246.
- (18) Behr, A.; Leschinski, J.; Awungacha, C.; Simic, S.; Knoth, T. *ChemSusChem* **2009**, *2*, 71–76.
- (19) In Lee, B.; Hee Lee, K.; Sung Lee, J. *J. Mol. Catal. A: Chem.* **2000**, *156*, 283–287.
- (20) Estrine, B.; Soler, R.; Damez, C.; Bouquillon, S.; Hémin, F.; Muzart, J. *Green Chem.* **2003**, *5*, 686–689.
- (21) Kaneda, K.; Kurosaki, H.; Terasawa, M.; Imanaka, T.; Teranishi, S. *J. Org. Chem.* **1981**, *46*, 2356–2362.
- (22) Benvenuti, F.; Corlini, C.; Raspolli Galletti, A. M.; Sbrana, G.; Marchionna, M.; Patrini, R. *J. Mol. Catal. A: Chem.* **1999**, *137*, 49–63.
- (23) Pittman, C. U., Jr.; Wu, S. U.; Jacobson, S. E. *J. Catal.* **1976**, *44*, 87–100.
- (24) Estrine, B.; Bouquillon, S.; Hémin, F.; Muzart, J. *Appl. Organomet. Chem.* **2007**, *21*, 946–946.
- (25) Wahlen, J.; De Vos, D. E.; Sels, B. F.; Nardello, V.; Aubry, J.-M.; Alsters, P. L.; Jacobs, P. A. *Appl. Catal. A: Gen.* **2005**, *293*, 120–128.
- (26) Constantino, U.; Marmottini, F.; Nocchetti, M.; Vivani, R. *Eur. J. Inorg. Chem.* **1998**, 1439–1446.
- (27) Neațu, F.; Besnea, M.; Kromvotkis, V. G.; Genêt, J.-P.; Michelet, V.; Triantafyllides, K. S.; Parvulescu, V. I. *Catal. Today* **2008**, *139*, 161–167.
- (28) Choudary, B. M.; Lakshmi Kantam, M.; Mahender Reddy, M.; Gupta, N. M. *Catal. Lett.* **2002**, *82*, 79–83.
- (29) Cavani, F.; Trifirò, F.; Vaccari, A. *Catal. Today* **1991**, *11*, 173–301.
- (30) Okamoto, K.; Sasaki, T.; Fujita, T.; Iyi, N. *J. Mater. Chem.* **2006**, *16*, 1608–1616.
- (31) Iosif, F.; Parvulescu, V. I.; Pérez-Bernal, M. E.; Ruano-Casero, R. J.; Rives, V.; Kranjc, K.; Polanc, S.; Kočevar, M.; Genin, E.; Genêt, J.-P.; Michelet, V. *J. Mol. Catal. A: Chem.* **2007**, *276*, 34–40.
- (32) Zhang, X.; Wei, M.; Pu, M.; Li, X.; Chen, H.; Evans, D. G.; Duan, X. *J. Solid State Chem.* **2005**, *178*, 2701–2708.
- (33) Terasawa, M.; Kaneda, K.; Imanaka, T.; Teranishi, S. *J. Organomet. Chem.* **1978**, *162*, 403–414.
- (34) Grenouillet, P.; Neibecker, D.; Poirier, J.; Tkatchenko, I. *Angew. Chem., Int. Ed.* **1982**, *21*, 767–768.
- (35) Bouachir, F.; Grenouillet, P.; Neibecker, D.; Poirier, J.; Tkatchenko, I. *J. Organomet. Chem.* **1998**, *569*, 203–215.
- (36) Schuchardt, U.; Nicolau Dos Santos, E.; Santo Dias, F. J. *Mol. Catal.* **1989**, *55*, 340–352.
- (37) Prihod'ko, R.; Sychev, M.; Kolomitsy, I.; Stobbelaar, P. J.; Hensen, E. J. M.; van Santen, R. A. *Microporous Mesoporous Mater.* **2002**, *56*, 241–255.
- (38) van Laar, F. M. P. R.; De Vos, D. E.; Pierard, F.; Kirsch-De Mesmaeker, A.; Fiermans, L.; Jacobs, P. A. *J. Catal.* **2001**, *197*, 139–150.
- (39) Corma, A.; Iborra, S. *Adv. Catal.* **2006**, *49*, 239–302.
- (40) Bjørgen, M.; Bonino, F.; Kolboe, S.; Lillerud, K.-L.; Zechina, A.; Bordiga, S. *J. Am. Chem. Soc.* **2003**, *125*, 15863–15868.
- (41) Benn, R.; Jolly, P. W.; Mynott, R.; Raspel, B.; Schenker, G.; Schick, K.-P.; Schroth, G. *Organometallics* **1985**, *4*, 1945–1953.
- (42) Jolly, P. W.; Mynott, R.; Raspel, B.; Schick, K. P. *Organometallics* **1986**, *5*, 473–481.
- (43) Szabó, K. J. *Chem.—Eur. J.* **2004**, *10*, 5268–5275.
- (44) Solin, N.; Kjellgren, J.; Szabó, K. J. *J. Am. Chem. Soc.* **2004**, *126*, 7026–7033.
- (45) Kiji, J.; Okano, T.; Nomura, T.; Saiki, K.; Sai, T.; Tsuji, J. *Bull. Chem. Soc. Jpn.* **2001**, *74*, 1939–1945.